

ELECTROMAGNETIC INTERFERENCE SHIELDING EFFECTIVENESS OF THE THIN CARBON NANOFIBERS/SILICON CARBIDE FABRICS COMPOSITES

Xiaojing JIA¹, Huan DU¹, Ligu ZHANG¹, Xinquan ZHANG¹ & Zhenquan ZHONG¹

¹ AVIC The first Aircraft Institute, Xi'an, Shaanxi 710089, PR China

Tel: +86-18009212005 Email: jiaxiaoter@126.com

Abstract

Slurry impregnation and chemical vapor deposition (CVD) method were used to prepare the thin carbon nanofibers/ silicon carbide fabrics (CNFs/SiC_f) composites. The microstructure, electrical conductivity, and electromagnetic interference (EMI) shielding effectiveness of CNF/SiC_f under different reaction times were investigated in detail. It can be shown that the slurry impregnation method could evenly introduce the catalyst layer and realize the effective dispersion of the catalyst. By exploring the growth process of CVD, 15 min was the best reaction time which could realize the combination of high quality and high loading quantity of carbon nanofibers (CNFs). At this time, CNFs had the good graphitization degree and the diameter was around 25 nm. The results showed that the higher the mass fraction of CNFs was, the better electrical conductivity and EMI shielding property over the frequency range of 8.2-12.4 GHz (X-band) could be obtained with the reaction time extending. The thin CNFs/SiC_f composites showed the excellent potential of EMI shielding material with highly absorbing performance.

Keywords: electromagnetic interference shielding, carbon nanofiber, silicon carbide, composite

1. Introduction

With the development of aviation technology, a new generation of aircraft put higher demands for supersonic speed and stealth [1]. Due to the aerodynamic heating caused by supersonic flight, the edge structures of stealth aircraft like the leading edge, trailing edge, and the tip of the wing or tail wing will suffer the higher temperature. Furthermore, the parts of the nozzle and afterdeck also put demands on high-temperature stealth materials. According to the different application forms, stealth materials can be divided into coatings and structure materials [2]. For the above-mentioned high-temperature stealth structures, coating and the substrate surface will have bad contraction stress under the repeated impact of high and low temperatures, leading to cracking and peeling. It also has the problems [3] of increase in weight and high maintenance costs, etc. Therefore, in the high-temperature working environment, the structure stealth materials are the ideal choice. They not only have more functions, such as thermal protection, stealth, and electromagnetic interference (EMI) shielding but also meet the mechanical requirements.

The most common structure stealth material is represented by continuous fiber-reinforced composites. The typical fibers include Kevlar fiber, quartz fiber, carbon fiber, and silicon carbide fiber. Compared to other fibers, silicon carbide fiber has relatively low density, excellent oxidation resistance, high strength retention at elevated temperature, and good thermal shock resistance, thus it has been widely used in high-temperature structural composites. On the other hand, silicon carbide fiber has a wide range of electrical resistance from 10^{-3} to $10^4 \Omega \cdot m$ by tailoring surface characteristics [4]. Due to this unique electromagnetic property, silicon carbide fiber can realize electromagnetic wave absorption or EMI shielding under high-temperature or harsh working environments. Reports [5-6] show that the surface modification of silicon carbide fiber by metal or carbon materials can achieve the adjustment of electric conductivity and exhibit better electromagnetic properties. But metal (such as nickel, iron, and cobalt) would damage the performance and increase the density of

silicon carbide fiber [5]. One-dimensional carbon nanomaterials such as carbon nanotubes (CNTs) and carbon nanofibers (CNFs) have excellent electrical conductivity, large aspect ratio, higher specific surface area, and lower density [7-10]. Therefore, silicon carbide fiber modified by CNFs is expected to be promising candidates for EMI shielding materials with high absorbing properties and the feature of thin thickness.

In this paper, two-dimensional layered silicon carbide fabrics (SiC_f) were used as the skeleton materials and the different loading of CNFs were obtained on the surface by slurry impregnation and chemical vapor deposition (CVD) method. Scanning electron microscopy (SEM), transmission electron microscopy (TEM), and X-ray diffraction (XRD) were utilized to characterize the structure and morphology of the CNF/SiC_f. The effects of different reaction times and mass fraction CNFs at 800 °C on electrical conductivity and EMI SE of CNF/SiC_f composites were investigated in detail.

2. Experimental procedures

2.1 Fabrication of CNF/SiC_f composites

Firstly, catalyst slurry was prepared. The phenolic resin (PF 2313, 96.5% purity), nano-sized Ni particles (mean diameters 30 nm, 99.9% purity), and nano-sized SiO₂ particles (mean diameters 10 nm, 99.9% purity) were dissolved in ethanol with the weight ratio of 3:3:1. After that, this catalyst slurry was under ultrasonication for 10min to form a homogeneous solution. In this process, phenolic resin, Ni particles, and SiO₂ particles are acted as adhesive, catalyst, and dispersant, respectively.

Secondly, the two-dimensional layered silicon carbide fabrics (2D SiC_f, 0.25 K, plain weave, made in Xiamen University) were selected as the substrate. Subsequently, the 2D SiC_f was dipped in catalyst slurry for the 30s. Then, put it on the filter paper and dried at room temperature for 30 min.

Thirdly, the as-prepared 2D SiC_f was used as preforms to grow CNFs in a horizontal tube furnace (Hefei Kejing Materials Technology Co, OTF-1200X) via the CVD method under 800 °C. Before growth, a 15 min heat treatment was prepared under H₂ (60 sccm) and Ar (120 sccm). Growth was started by flowing C₂H₄ gas (60 sccm) in the furnace at ambient pressure. The reaction time was 5, 10, 15, and 20 min, respectively. Then, the furnace was gradually cooled to ambient temperature under Ar (120 sccm). To prepare the testable composites, CNF/SiC_f was mixed with paraffin and cold-pressed into green bodies under a pressure of 5 MPa. Then cut the composites into the measurement samples with the dimension of 22.86×10.16×0.28 mm³ for the measurement of electromagnetic interference shielding effectiveness (EMI SE).

2.2 Characterization

The morphology of the CNF/SiC_f was investigated by Scanning electron microscopy (SEM, S-4700, Hitachi, 15 kV). SEM uses the focused beam of high-energy electrons to scan the samples. Through the interaction between the beam and the sample, it collects, enlarges, and re-images to characterize the microscopic morphology of the materials. The microstructure of the CNF/SiC_f was observed by Transmission Electron Microscope (TEM, G-20, FEI-Tecnai, 200 kV). Compared with the SEM, TEM has the higher resolution and it also can obtain the degree of crystallization of the sample. For TEM observations, the CNF/SiC_f composites were ultrasonically dispersed in ethanol for 30 min and then dropped onto a TEM grid. X-ray diffraction (XRD) is widely used for phase and crystal structure analysis. The crystal structure of the as-synthesized sample was identified by XRD (X' Pert Pro, Philips) to obtain the phase and crystallization, using Cu Kα (λ=1.54 Å) radiation. Electrical conductivity was measured by the two-wire method using a current source (Keithley 6220 DC; Ohio, USA). The electromagnetic interference shielding property was evaluated by scattering parameters [11]. The scattering parameters (S₁₁ and S₂₁) of the as-received samples with the dimension of 22.86×10.16×0.28 mm³ were measured by a vector network analyzer (VNA, MS4644A, Anritsu, Atsugi, Japan) using the wave-guide method in the frequency range 8.2–12.4 GHz (X-band).

3. Results and Discussions

3.1 Uniformly controlled catalyst distribution

In the heat treatment process, the phenolic resin of the slurry was gradually consumed and the encapsulated catalyst was gradually released. After heat treatment, the morphology and distribution of catalyst nanoparticles on the SiC_f surface were observed by SEM as shown in Fig.1 (a-b). In Fig.1 (a), the low magnification SEM shows that the surface of SiC_f was uniformly covered by the catalyst

layer. And the uniformity was not an occasion but existed in a wide range. In Fig.1 (b), it can be observed that the thickness of the catalyst layer was about 150 nm and the sizes of the catalyst particles were between 10 nm and 70 nm which were consistent with the sizes of the selected Ni particles. It is shown from Fig.1 that the slurry impregnation method could evenly introduce the catalyst layer and realized the effective dispersion of the catalyst.

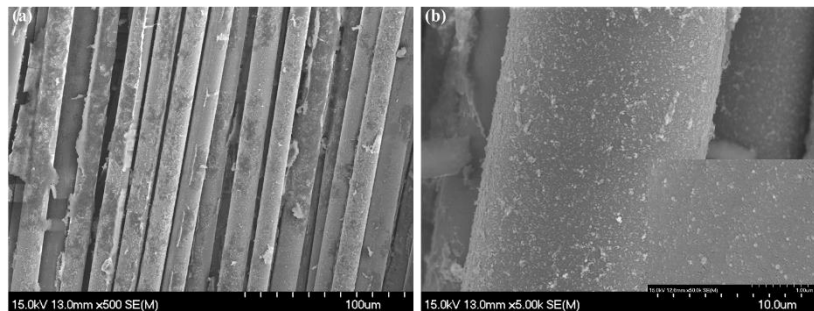


Figure 1 –The SEM of SiC_f after heat treatment.

3.2 Morphology and microstructure of CNFs/ SiC_f

Fig. 2 shows the SEM of CNFs/SiC_f at different reaction times under 800 °C. In Fig.2 (a-d), CNFs were in-situ growth on the SiC_f surface uniformly. With the extension of reaction time, the boundaries were not obvious and the bridges were formed between fiber and fiber. When the reaction time was under 15 min, it can be seen that the diameters of CNFs were around 25 nm (Fig.2 (e)). However, when the reaction time reached 20min, the amorphous carbon deposited on the surface of CNFs is shown in Fig.2 (f). The reason for this phenomenon is that the effective sites of the catalyst were completely occupied which led to losing the activity of the catalyst. Instead of producing CNFs, the surplus carbon source was deposited on the surface of CNFs in the form of amorphous carbon.

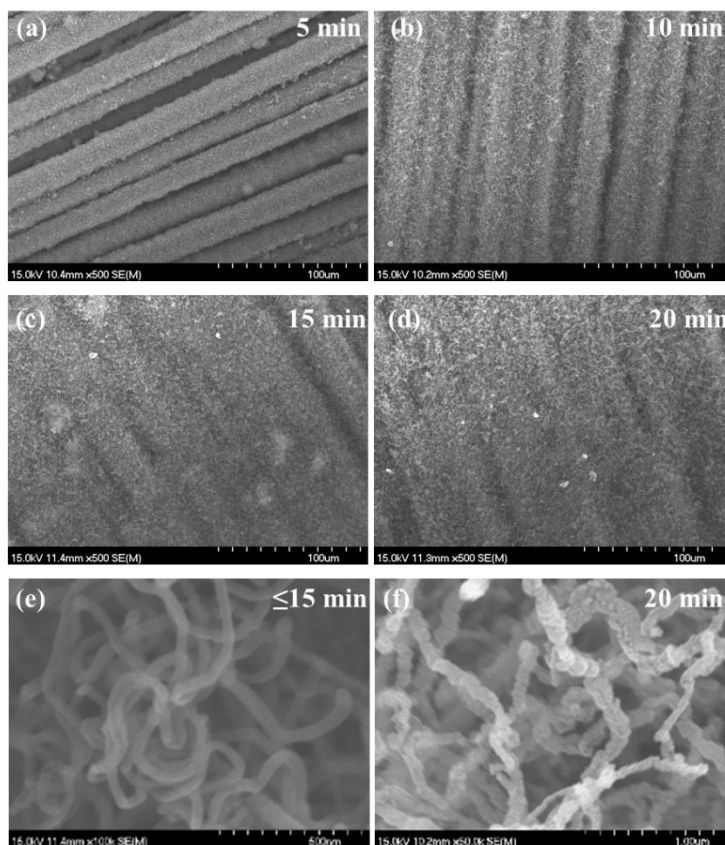


Figure 2 –The SEM of CNFs/SiC_f in different reaction times.

3.3 Morphology and microstructure of CNFs/ SiC_f

Table 1 shows the percentage of weight gain of CNFs/SiC_f in different reaction times. After 5, 10, 15, and 20 min, the percentage of weight gain were 2.03 wt.%, 4.08 wt.%, 6.24 wt.%, and 6.93wt.%, respectively. The percentage of weight gain increased with the increase in reaction time. When the growth time was under 15 min, the percentage of weight gain was almost proportional to the reaction time. When the growth time reached 20 min, the percentage of weight gain increased too, but more slowly and slightly. According to Fig. 2 and Table 1, it can be concluded that 15 min was the best reaction time which could realize the combination of the high quality and the high loading quantity of CNFs. So, we selected this sample to characterize the microstructures.

Table 1 – Percentage of weight gain of CNFs/SiC_f in different reaction times.

SiC _f	5min	10min	15min	20min
Original weight (g)	0.1431	0.1519	0.1570	0.1719
Weight after growth (g)	0.0029	0.0062	0.0098	0.0129
Percentage of weight gain (wt.%)	2.03	4.08	6.24	6.93

TEM and XRD were employed to analyze the microstructures of CNFs/SiC_f (Fig. 3). Different from the typical hollow structure of CNT, the TEM images in Fig. 3(a-b) show that those carbon nanostructures were solid which demonstrated the carbon nanostructures were CNFs. It can be seen that the diameter of CNFs were around 25 nm and the catalyst were on the top. The electron diffraction pattern showed Debye rings, which indicated that the CNFs had good graphitization degree.

Fig. 3 (c) shows the XRD patterns of SiC_f and CNFs/ SiC_f samples. For as-received SiC_f, three diffraction peaks near the 2θ of 35.6°, 60.0°, and 71.8° corresponded to the (111), (220), and (311) crystal planes of β-SiC respectively, and β-SiC had a preferred growth along (111) crystal plane orientation in view of its highest peak intensity. In addition, a peak of the C (002) plane at 2θ of 26.5° appeared. It indicated that the SiC_f comprises turbostratic carbon which led to lower electrical resistivity. After growth, the intensity of this carbon peak increased significantly. It is known that higher intensity of the C (002) peak is indicative of improved graphitic degree [12]. According to the XRD patterns, it can be concluded that the as-prepared CNFs had good graphitization degree which was consistent with the TEM diffraction pattern.

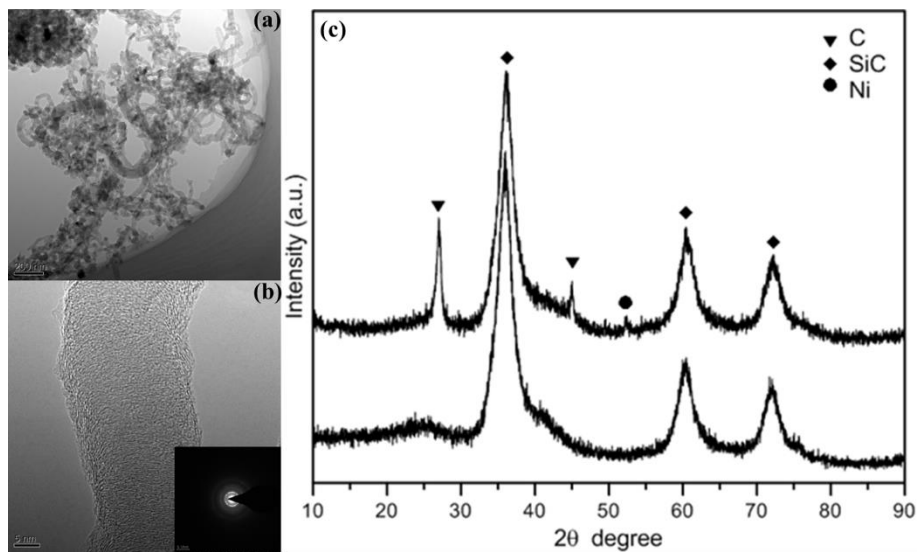


Figure 3 –The TEM and XRD of CNFs under 800°C

3.4 Electrical conductivity of CNFs/ SiC_f

Generally considered, the EMI SE goes up in proportion to the electrical conductivity, namely: a rise

in conductivity will create increased EMI SE. Therefore, conductivity can play a guiding role in EMI SE. When the materials have low porosity, researchers tend to use a surface electrical conductivity to characterize the shielding effectiveness. In contrast, when the materials have large porosity, most of the incident power enters the material through the open pores. In this circumstance, it will be more reasonable to employ a volume resistance measured with the two-wire method to characterize the electromagnetic properties [13]. Based on Ohm's law, the electrical conductivity can be calculated as follow:

$$\delta = l/RS \quad (1)$$

where δ is the electrical conductivity of the material, R is the measured resistance, and S and l are the cross-sectional area and length of the sample, respectively.

Table 2 – Percentage of weight gain and electrical conductivity of CNFs/SiC_f in different reaction times.

	0min	5min	10min	15min	20min
Conductivity (S/m)	1.685	31.123	66.148	93.985	97.261
Percentage of weight gain (wt.%)	0	2.03	4.08	6.24	6.93

Table 2 shows the changes in room temperature electrical conductivity and percentage of weight gain of CNFs/SiC_f in different reaction times. For 2D layered silicon carbide fabrics, current transfer only passed through the intersection points of the warp yarn and the weft yarn. So, the electrical conductivity of the as-received sample was just 1.685 S/m. After growth, CNFs provided additional paths for the electrical current which led to increases in electrical conductivity. Combining the data in Table 2 and Fig. 4, it can be seen that the conductivity increased sharply from 1.685 to 93.985 S/m, then increased slightly to 97.261 S/m after growth for 20 min. The results indicated that the variation tendency of conductivity with reaction time was as same as the tendency of the percentage of weight gain with reaction time. When the reaction time was under 15 min, the conductive and the percentage of weight gain were in proportion to the reaction time. In contrast, when the reaction time was over 15 min, both increased slightly. The reason for this phenomenon was that instead of CNFs, the amorphous carbon just could make a little contribution to the improvement of electrical conductivity.

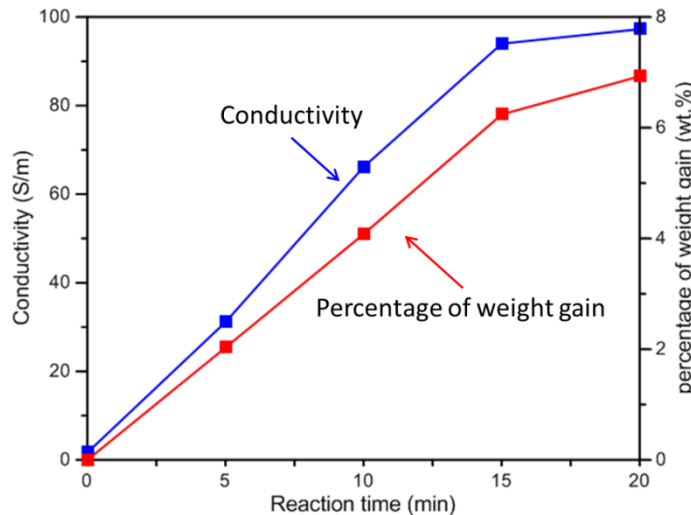


Figure 4–Percentage of weight gain and electrical conductivity of CNFs/SiC_f in different reaction times.

3.5 EMI SE of CNF/SiC_f composites

According to Schelkunoff's theory, the total shielding (SE_T) is determined by absorption loss (SE_A), reflection loss (SE_R), and multiple reflections (SE_M) together. That is:

$$SE_T = SE_A + SE_R + SE_M \quad (2)$$

EMI is attenuated by three major mechanisms, namely: reflection, absorption, and multiple reflections. Multiple reflections are the internal reflections between the internal surfaces of the shielding material. In cases where the shielding by absorption (i.e., absorption loss) is higher than 10 dB, most of the re-reflected wave will be absorbed within the shield [14]. Thus, multiple reflections can be ignored. The formula (2) can be simplified as follow:

$$SE_T \approx SE_A + SE_R \quad (3)$$

In the actual measurement process, S-parameters were used to calculate the EMI SE. SE_A and SE_R were calculated based on the S-parameters obtained from the vector network analyzer as follows:

$$SE_A = -10 \log[T/(1 - R)] \quad (4)$$

$$SE_R = -10 \log(1 - R) \quad (5)$$

where $R = |S_{11}|^2 = |S_{22}|^2$, $T = |S_{12}|^2 = |S_{21}|^2$, $A=1-T-R$.

Fig. 5 shows the EMI SE of CNFs/SiC_f composites under different reaction times during X-band. It can be seen that EMI SE was shielded mainly by absorption and the values of SE_T , SE_R , and SE_A of these composites increased with reaction time. Before growth, the SE_T , SE_A , and SE_R were 7.5 dB, 5.3 dB, and 2.2 dB, respectively. It was beneficial to the decrease of the reflected waves, due to the electrical conductivity of the sample (1.685 S/m) would be much smaller than that of metals. Fig.5 (a) shows that with the increase in reaction time, SE_T enhanced which was in good agreement with the increase of conductivity. The EMI SE of SiC_f increased with the increasing loading of CNFs, because of forming the CNFs conductive network on the surface of SiC_f. The introduction of CNFs may increase the concentration of carriers. As a result, the SE_T increased significantly from 7.5 dB to 17.8 dB at 10 GHz with the formation of CNFs (6.24 wt. %). This increase mainly came from the increase in SE_A . And SE_A was always much higher than SE_R during X-band. The SE_A increased significantly from 5.3 dB to 12.0 dB and the SE_R increased from 2.2 dB to 5.8 dB at 10 GHz. When the reaction time is greater than 15 min, SE_T is larger than 15 dB which indicated that SiC_f modified by CNFs can obtain high EMI SE with thin thickness. And the higher the mass fraction of CNFs was, the better SE_A could be obtained.

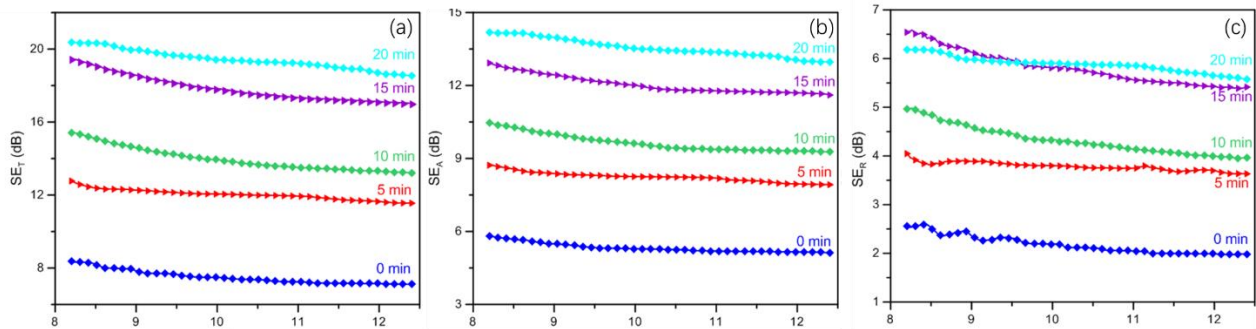


Figure 5—EMI SE of CNFs/SiC_f composites under different reaction times during X-band.

(a) SE_T ; (b) SE_A ; (c) SE_R

4. Conclusions

A uniformly controlled catalyst layer was obtained by slurry impregnation on the surface of SiC_f and CNFs were in situ grown via the CVD method. At 15 min, the best morphology of CNFs was obtained. The electrical conductivity and EMI SE of SiC_f before and after growth was investigated over the frequency range of 8.2-12.4 GHz (X-band). The results show that the higher the mass fraction of CNFs was, the better electrical conductivity and EMI shielding property could be obtained with the reaction time extension. And the thin CNFs/SiC_f composites show the excellent potential of EMI shielding material with highly absorbing performance.

References

- [1] altzman E J , Ayers T G . Selected Examples of NACA/NASA Supersonic Flight Research. 1995.
- [2] Chen K , Zeng H B , Hui H U . Radar stealth material study[J]. Modern Defense Technology, 2005.
- [3] Zhao, Jiaxiang. Silicon carbide fiber and its composite materials [J]. High-tech fibers & application, 2002, 27(4):7.

- [4] Ye F, Zhang L, Yin X, et al. Dielectric and Electromagnetic Wave Absorbing Properties of Two Types of SiC Fibres with Different Composition[J]. *Journal of Materials Science & Technology*, 2013.
- [5] H.F. Cheng, Z.H. Chen, Y.Q. Li, C.R. Zhang, D. Wang, Improvement of electromagnetic parameters of chopped SiC fibers, *Aerosp. Mater. Technol.* 29 (1999) 41-44
- [6] Zhang, Litong, Cheng, et al. Flexible thin SiC fiber fabrics using carbon nanotube modification for improving electromagnetic shielding properties[J]. *Materials & design*, 2016.
- [7] Rahaman M, Chaki T K, Khastgir D. High - performance EMI shielding materials based on short carbon fiber - filled ethylene vinyl acetate copolymer, acrylonitrile butadiene copolymer, and their blends[J]. *Polymer Composites*, 2011, 32(11): 1790-1805.
- [8] Jou W S, Cheng H Z, Hsu C F. The electromagnetic shielding effectiveness of carbon nanotubes polymer composites[J]. *Journal of Alloys and Compounds*, 2007, 434: 641-645.
- [9] Mazov I, Kuznetsov V, Moseenkov S, et al. Electromagnetic shielding properties of MWCNT/PMMA composites in Ka-band[J]. *Physica Status Solidi*, 2009, 246(246):2662-2666.
- [10] Micheli D, Apollo C, Pastore R, et al. X-Band microwave characterization of carbon-based nanocomposite material, absorption capability comparison and RAS design simulation[J]. *Composites Science & Technology*, 2010, 70(2):400-409.
- [11] Micheli D, Apollo C, Pastore R, et al. Optimization of Multilayer Shields Made of Composite Nanostructured Materials[J]. *IEEE Transactions on Electromagnetic Compatibility*, 2012, 54(1):60-69.
- [12] Lawrence, E, Crooks. Noise reduction techniques in electronic systems (2nd ed.), Henry W. Ott. Wiley-Interscience, New York. 1988[J]. *Magnetic Resonance in Medicine*, 1989..
- [13] Luo K , Yin X , Yuan X , et al. Electromagnetic wave absorption properties of graphene modified with carbon nanotube/poly(dimethyl siloxane) composites[J]. *Carbon*, 2014, 73:185-193.
- [14] Lovat G . *Electromagnetic Shielding*[J]. Springer New York, 2007.

Copyright Statement

The authors confirm that they, and/or their company or organization, hold copyright on all of the original material included in this paper. The authors also confirm that they have obtained permission, from the copyright holder of any third party material included in this paper, to publish it as part of their paper. The authors confirm that they give permission, or have obtained permission from the copyright holder of this paper, for the publication and distribution of this paper as part of the ICAS proceedings or as individual off-prints from the proceedings.